

*Short note*

## Improved information on electron screening in ${}^7\text{Li}(p, \alpha)\alpha$ using the Trojan-horse method

 M. Aliotta<sup>1,a</sup>, C. Spitaleri<sup>2</sup>, M. Lattuada<sup>2</sup>, A. Musumarra<sup>2</sup>, R.G. Pizzone<sup>2</sup>, A. Tumino<sup>3</sup>, C. Rolfs<sup>1,b</sup>, and F. Strieder<sup>1</sup>
<sup>1</sup> Institut für Physik mit Ionenstrahlen, Ruhr-Universität Bochum, Germany

<sup>2</sup> Dipartimento di Metodologie Fisiche e Chimiche per l'Ingegneria dell'Università di Catania and INFN - Laboratori Nazionali del Sud, Catania, Italy

<sup>3</sup> Dipartimento di Fisica e Astronomia dell'Università di Catania and INFN - Laboratori Nazionali del Sud, Catania, Italy

Received: 9 September 2000 / Revised version: 14 November 2000

Communicated by J. Äystö

**Abstract.** The available astrophysical  $S(E)$  factor data for the reaction  ${}^7\text{Li}(p, \alpha)\alpha$  at  $10 < E < 1000$  keV exhibit an exponential increase at low energies due to the effects of electron screening. A parametrisation of the data using a non-resonant, direct process and two subthreshold resonances reproduces the data at energies  $E \geq 100$  keV, while at lower energies this calculated  $S_b(E)$  factor curve for bare nuclides drops below the data, which in turn represent the case of electron-shielded nuclides, *i.e.* the electron-shielded  $S_s(E)$  factor. The comparison between  $S_b(E)$  and  $S_s(E)$  leads to an electron-screening potential energy  $U_e = 350$  eV, which is much higher than the adiabatic limit of 175 eV and not understood at present. The deduced value of  $S_b(0)$  is considerably smaller than the previously adopted value of 59 keV b, significantly increasing the calculated abundance of  ${}^7\text{Li}$  in big-bang nucleosynthesis. The Trojan-horse method was applied to the reaction  ${}^7\text{Li}(p, \alpha)\alpha$  to determine the energy dependence of the  $S_b(E)$  factor for  $10 < E < 370$  keV, free from the effects of the Coulomb barrier and electron screening. The THM results are close to the calculated  $S_b(E)$  curve and suggest that the THM may become a powerful way to obtain improved information on low-energy cross-sections and associated electron-screening effects in a model-independent way.

**PACS.** 24.10.-i Nuclear-reaction models and methods – 25.40.-h Nucleon-induced reactions – 26.35.+c Big bang nucleosynthesis

Accurate knowledge of thermonuclear reaction rates is important for the field of nuclear astrophysics [1,2]. Due to the Coulomb barrier of the entrance channel, the cross-section  $\sigma(E)$  of these fusion reactions drops exponentially with decreasing center-of-mass energy  $E$ ,

$$\sigma(E) = S(E)E^{-1} \exp(-2\pi\eta), \quad (1)$$

where  $\eta$  is the Sommerfeld parameter and  $S(E)$  is the astrophysical  $S$ -factor. The parametrisation assumes that the Coulomb barrier is that resulting from bare nuclei. However, for nuclear reactions studied in the laboratory, the target nuclei and the projectiles are usually in the form of neutral atoms or molecules and ions, respectively. The resulting enhancement of the electron-screened cross-section,  $\sigma_s(E)$ , over that for bare nuclei,  $\sigma_b(E)$ , is de-

scribed by the expression [3–5]

$$f_{\text{lab}}(E) = \sigma_s(E)/\sigma_b(E) = S_s(E)/S_b(E) = (E/E + U_e) \exp(\pi\eta U_e/E), \quad (2)$$

where  $U_e$  is the constant electron-screening potential energy, and  $S_s(E)$  and  $S_b(E)$  refer to the respective  $S$ -factor for screened and bare nuclides. Note that  $f_{\text{lab}}(E)$  increases exponentially with decreasing energy. For ratios  $E/U_e > 1000$ , shielding effects are negligible, and laboratory experiments can be regarded as essentially measuring  $\sigma_b(E)$ . However, for  $E/U_e < 100$ , shielding effects become important: even relatively small enhancements from electron screening at energy ratios  $E/U_e = 100$  can cause significant errors in the extrapolation of cross-sections to lower energies, if the curve of the cross-section is forced to follow the trend of the enhanced cross-sections, without correction for the screening. Note that for a stellar plasma the value of  $\sigma_b(E)$  must be known because the screening in the plasma will be quite different from that in

---

<sup>a</sup> Alexander von Humboldt Fellow

<sup>b</sup> e-mail: rolfs@ep3.ruhr-uni-bochum.de

the laboratory nuclear-reaction studies, *i.e.*  $\sigma_{\text{plasma}}(E) = f_{\text{plasma}}(E)\sigma_b(E)$ , and  $\sigma_b(E)$  must be explicitly included at each energy. A good understanding of electron-screening effects is needed to arrive at reliable  $S_b(E)$  data at low energies, and may also help to improve the corresponding understanding of electron screening in a stellar plasma.

The exponential enhancement has been observed in several fusion reactions [6–14], at energies from a few keV to a few tens of keV (in the following we refer to these data as “standard”). However, the observed enhancements were much larger than the adiabatic limit, *i.e.*, the difference in electron binding energies between the colliding atoms and the compound atom. The most pronounced excess has been reported for the  ${}^3\text{He}(d,p){}^4\text{He}$  reaction,  $U_e = 186 \pm 9 \text{ eV}$  [9], significantly larger than the adiabatic limit  $U_e = 120 \text{ eV}$ . A solution to the larger than expected values of  $U_e$  might be found in one or more of the following areas: i) the assumed energy loss predictions from stopping-power codes at low energies (*e.g.*, [14–17] for the  $d+{}^3\text{He}$  system), ii) the assumed nuclear-reaction models at energies far below the Coulomb barrier, and iii) the assumed atomic-physics models. All of these areas require additional experimental and theoretical efforts.

The  ${}^7\text{Li}(p,\alpha)\alpha$  reaction was studied—in the standard way—using a proton beam and a  ${}^7\text{Li}$  solid target as well as a  ${}^7\text{Li}$  beam and a  $\text{H}_2$  gas target ([7, 18] and references therein), where the resulting data are displayed in fig. 1. A theoretical analysis of the data is missing, although it was suggested [19] that such an analysis may have to include a non-resonant, direct process as well as two  $J^\pi = 2^+$  subthreshold resonances at  $E_{R1} = -0.62 \text{ MeV}$  and  $E_{R2} = -0.33 \text{ MeV}$  with total widths  $\Gamma_{R1} = 108 \text{ keV}$  and  $\Gamma_{R2} = 74 \text{ keV}$  ( ${}^8\text{Be}$  states at 16.63 and 16.92 MeV excitation energy). We have followed this suggestion in a simple parametrisation of the data. Firstly, the reaction can only proceed via  $p$ -waves in the entrance channel. For a non-resonant, direct process (DP) alone, the  $p$ -wave centrifugal barrier leads to an  $S(E)$  factor falling much steeper than the data (dotted curve in fig. 1). We included thus the two  $p$ -wave subthreshold resonances and the associated interference terms:

$$S_b(E) = S_{\text{DP}}(E) + S_{R1}(E) + S_{R2}(E) \\ \pm 2(S_{R1}(E)S_{R2}(E))^{1/2} \cos \Phi_{R1,R2} \\ \pm 2(I_R S_{\text{DP}}(E)S_{R1}(E))^{1/2} \cos \Phi_{\text{DP},R1} \\ \pm 2(I_R S_{\text{DP}}(E)S_{R2}(E))^{1/2} \cos \Phi_{\text{DP},R2},$$

where the non-resonant, direct process is described by  $S_{\text{DP}}(E) = NP_{l=1}(E)/P_{l=0}(E)$  ( $P_l(E)$  = penetrability for  $s$ - and  $p$ -waves;  $N$  = free parameter) and the high-energy tail of each subthreshold resonance is parametrised by a Breit-Wigner expression [2], with the reduced proton width  $\theta_{l=1}^2$  taken as free parameter. The resonance phase is described by  $\Phi_{Ri}(E) = \arctan(0.5\Gamma_{Ri}(E)/(E - E_{Ri}))$ , where the energy dependence of the total width includes the contributions of both the proton- and alpha-channels, leading to  $\Phi_{\text{DP},Ri} = \Phi_{Ri}$  and  $\Phi_{R1,R2} = \Phi_{R1} - \Phi_{R2}$ . Finally, the factor  $I_R = 5/16$  represents a statistical fac-

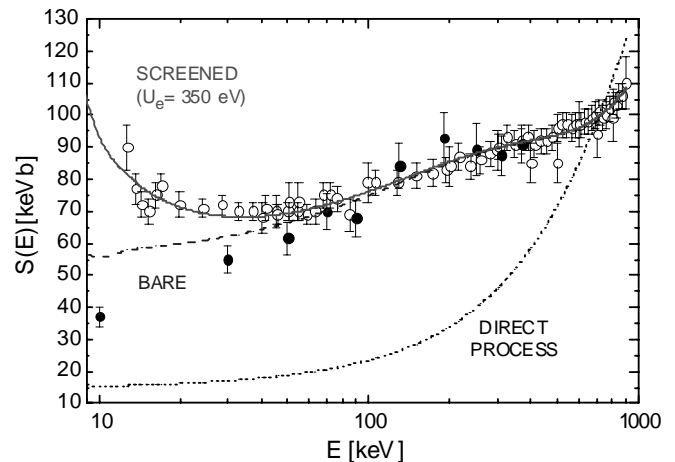


**Fig. 1.** Astrophysical  $S$ -factor of shielded nuclides,  $S_s(E)$ , for the reaction  ${}^7\text{Li}(p,\alpha)\alpha$  as obtained by standard measurements (standard data = open circles). The dotted curve represents the  $S$ -factor  $S_b(E)$  (bare nuclides) for a  $p$ -wave non-resonant, direct process alone. The dashed curve is the  $S_b(E)$ -result of a fit to the standard data at  $E \geq 100 \text{ keV}$  using the non-resonant, direct process and two subthreshold resonances. The solid curve is the  $S$ -factor for screened nuclei derived from eq. (2) with  $U_e = 350 \text{ eV}$  together with the  $S_b(E)$  dashed curve. The data obtained by the Trojan-horse method (filled circles) support the trend in the energy dependence of the calculated  $S_b(E)$  curve.

tor between the  $J^\pi = 2^+$  resonances and the possible angular momenta of the non-resonant, direct process ( $J^\pi = 0^+$  to  $3^+$ ). A fit to the data at energies  $E \geq 100 \text{ keV}$  (*i.e.*, no significant effects of electron screening expected) leads to the dashed curve in fig. 1, for the parameters  $N = 0.55$ ,  $\theta_{l=1}^2(R1) = 1.04$ ,  $\theta_{l=1}^2(R2) = 0.13$ , and the sign-combination  $--+$  of the 3 interference terms. At zero energy one finds  $S_b(0) \approx 40 \text{ keV b}$ , which may be compared with the adopted value  $S_b(0) = 59 \text{ keV b}$  [7, 18]. An improved analysis is highly desirable since the present low  $S_b(0)$  value leads to a higher calculated  ${}^7\text{Li}$  abundance in big-bang nucleosynthesis [1, 2] influencing the conclusions on the universal baryon density. Assuming the validity of the calculated  $S_b(E)$  curve, a comparison with the standard data at  $E \leq 100 \text{ keV}$  leads to  $U_e = 350 \text{ eV}$  (solid curve in fig. 1). This value is substantially higher than the adiabatic limit (175 eV) and is not understood at present. Since the standard measurements have also been carried out in inverted kinematics with nearly identical results [7], it is unlikely that the data are heavily influenced by incorrect energy-loss values.

A possible way to test the calculated  $S_b(E)$  curve (*i.e.* area ii) from above) is the so-called Trojan-horse method (THM), which allows one to measure the energy dependence  $S_b(E)$  down to the relevant low energies, free of the effects of the Coulomb barrier and electron screening. The principle of the THM has been discussed previously ([20] and references therein). Briefly, a particle  $a$  strikes a nucleus  $A$ , where  $A$  is described by a wave function with a large amplitude for a  $s$ - $b$  cluster configuration. Under

appropriate kinematic conditions the particle  $a$  then interacts only with the part  $b$  of the target nucleus  $A$ , while the other part  $s$  behaves as a spectator to the process  $a + b(+s) \rightarrow c + d(+s)$ . In order to completely determine the kinematic properties of the spectator  $s$ , the energies  $E_c$  and  $E_d$  of the two particles  $c$  and  $d$  must be measured in coincidence at specific angles  $\theta_c$  and  $\theta_d$ , respectively. In the plane-wave impulse approximation the three-body cross-section may be expressed as

$$d^3\sigma/dE_c d\Omega_c d\Omega_d \propto (\text{KF})|\Phi(p_s)|^2 d\sigma^N/d\Omega, \quad (3)$$

where KF is a kinematic factor containing the final-state phase-space factor,  $|\Phi(p_s)|^2$  is the momentum distribution of the spectator  $s$  inside the nucleus  $A$ , and  $d\sigma^N/d\Omega$  is the differential nuclear cross-section for the reaction  $a + b \rightarrow c + d$ . With the known terms KF and  $|\Phi(p_s)|^2$  one can derive  $d\sigma^N/d\Omega$  from a measurement of  $d^3\sigma/dE_c d\Omega_c d\Omega_d$ , whereby integration over the solid angle leads finally to the total cross-section  $\sigma^N(E)$ . Furthermore, if the bombarding energy is chosen to be above the Coulomb barrier in the incident channel of the reaction  $a + A \rightarrow c + d + s$ , the particle  $b$  can be brought into the nuclear interaction zone to induce the reaction  $a + b \rightarrow c + d$ . If the Fermi motion of particle  $b$  inside  $A$  compensates at least in part for the initial projectile velocity  $v_a$ , the reaction  $a + b \rightarrow c + d$  can be induced at a low relative energy between  $a$  and  $b$ , relevant to nuclear astrophysics. Note that the deduced reaction cross-section  $\sigma^N(E)$  is the nuclear part alone, since the Coulomb barrier has already been overcome in the entrance channel. The corresponding astrophysical  $S^N(E)$  factor is then derived from the relation  $S^N(E) = E\sigma^N(E)$  [20], where  $S^N(E)$  represents the  $S$ -factor for bare nuclides, since the projectile energy is above the height of the Coulomb barrier for the entrance channel. Since  $S(E)$  as defined by eq. (1) contains the term  $\exp(2\pi\eta)$  representing approximately the tunneling through the Coulomb barrier (for  $s$ -waves), a comparison of  $S^N(E)$  with the  $S(E)$  factor data from standard measurements requires the introduction of the term  $\exp(2\pi\eta)$  and the actual transmission factor  $T_{l=0}(E)$ ,

$$S_b(E) = S^N(E)T_{l=0}(E) \exp(2\pi\eta). \quad (4)$$

The absolute scale for  $S_b(E)$  is obtained by normalisation of the THM data to the standard data at energies where the effects of electron screening are negligible. Thus, the energy dependence of  $S_b(E)$  should be identical to that derived by the standard measurements, except at low energies, where the two data sets should differ due to the effects of electron screening. In turn, the value of  $U_e$  can then be obtained in a model-independent way by comparing the two data sets.

The  ${}^7\text{Li}(p, \alpha)\alpha$  reaction was studied with THM, *i.e.* using the reaction  ${}^2\text{H}({}^7\text{Li}, \alpha\alpha)n$  ( $A \equiv p$ - $n$  cluster,  $s \equiv n$  = spectator) [20–22]. The observed energy dependence of the broad resonance structures for  $1 < E < 7$  MeV [18] was well reproduced by the corresponding THM data [21]. The present THM data (fig. 1) differ somewhat from those reported previously [20, 22]: new data with higher statistical accuracy have been obtained and the normalisation

to the direct data has been carried out in the energy region  $E = 100$  to  $370$  keV. At energies above  $E = 100$  keV the standard and THM data agree within errors (after normalising), supporting the validity of the THM (see [21] for  $E \geq 1$  MeV), while at lower energies the THM data appear to support the trend in energy dependence of the calculated  $S_b(E)$  curve for bare nuclides. It should be noted that the THM data were obtained assuming a dominant  $p$ -wave contribution, which needs to be verified experimentally (such as done in the case of the reaction  ${}^6\text{Li}(d, \alpha)\alpha$  [23]).

Although it is not yet clear that all relevant components of the THM have been included in current analyses, the present work demonstrates how well the THM and standard measurements complement one another in determining both low-energy cross-sections and associated electron-screening effects. Further work on the theoretical aspects of the THM and on comparisons with low-energy data, as well as improved experimental data on low-energy energy loss, are urgently needed before one can have complete confidence in applying the THM to the problem of determining astrophysically important nuclear reaction cross-sections.

The authors thank C.A. Barnes for comments on the manuscript, and G. Baur, H.H. Wolter, and S. Typel for continuous support on the theoretical analyses.

## References

1. W.A. Fowler, *Rev. Mod. Phys.* **56**, 149 (1984).
2. C. Rolfs, W.S. Rodney, *Cauldrons in the Cosmos* (University of Chicago Press, 1988).
3. H.J. Assenbaum, K. Langanke, C. Rolfs, *Z. Phys. A* **327**, 461 (1987).
4. T.D. Shoppa, S.E. Koonin, K. Langanke, R. Seki, *Phys. Rev. C* **48**, 837 (1993).
5. G. Fiorentini, R.W. Kavanagh, C. Rolfs, *Z. Phys. A* **350**, 289 (1995).
6. S. Engstler *et al.*, *Phys. Lett. B* **202**, 179 (1988).
7. S. Engstler *et al.*, *Z. Phys. A* **342**, 471 (1992).
8. C. Angulo *et al.*, *Z. Phys. A* **345**, 231 (1993).
9. P. Prati *et al.*, *Z. Phys. A* **350**, 171 (1994).
10. U. Greife *et al.*, *Z. Phys. A* **351**, 107 (1995).
11. D. Zahnnow *et al.*, *Z. Phys. A* **359**, 211 (1997).
12. M. Junker *et al.*, *Phys. Rev. C* **57**, 2700 (1998).
13. R. Bonetti *et al.*, *Phys. Rev. Lett.* **82**, 5205 (1999).
14. H. Costantini *et al.*, *Phys. Lett. B* **482**, 43 (2000).
15. K. Langanke, T.D. Shoppa, C.A. Barnes, C. Rolfs, *Phys. Lett. B* **369**, 211 (1996).
16. J.M. Bang, L.S. Ferreira, E. Maglione, J.M. Hansteen, *Phys. Rev. C* **53**, R18 (1996).
17. R. Golser, D. Semrad, *Phys. Rev. Lett.* **66**, 1831 (1991).
18. C. Angulo *et al.*, *Nucl. Phys. A* **656**, 3 (1999).
19. C. Rolfs, R.W. Kavanagh, *Nucl. Phys. A* **455**, 179 (1986).
20. C. Spitaleri *et al.*, *Phys. Rev. C* **60**, 55802 (1999).
21. M. Zadro *et al.*, *Phys. Rev. C* **40**, 181 (1989).
22. G. Calvi *et al.*, *Nucl. Phys. A* **621**, 139 (1997).
23. S. Cherubini *et al.*, *Astrophys. J.* **457**, 855 (1996).